Development 135, 3665-3675 (2008) doi:10.1242/dev.027060

MEX-5 asymmetry in one-cell *C. elegans* embryos requires PAR-4- and PAR-1-dependent phosphorylation

Jennifer R. Tenlen[1,2,*], Jeffrey N. Molk[2,†], Nitobe London[2,3,†], Barbara D. Page[2,3] and James R. Priess[1,2,3,4,‡]

Anteroposterior polarity in early *C. elegans* embryos is required for the specification of somatic and germline lineages, and is initiated by a sperm-induced reorganization of the cortical cytoskeleton and PAR polarity proteins. Through mechanisms that are not understood, the kinases PAR-1 and PAR-4, and other PAR proteins cause the cytoplasmic zinc finger protein MEX-5 to accumulate asymmetrically in the anterior half of the one-cell embryo. We show that MEX-5 asymmetry requires neither vectorial transport to the anterior, nor protein degradation in the posterior. MEX-5 has a restricted mobility before fertilization and in the anterior of one-cell embryos. However, MEX-5 mobility in the posterior increases as asymmetry develops, presumably allowing accumulation in the anterior. The MEX-5 zinc fingers and a small, C-terminal domain are essential for asymmetry; the zinc fingers restrict MEX-5 mobility, and the C-terminal domain is required for the increase in posterior mobility. We show that a crucial residue in the C-terminus, Ser 458, is phosphorylated in vivo. PAR-1 and PAR-4 kinase activities are required for the phosphorylation of S458, providing a link between PAR polarity proteins and the cytoplasmic asymmetry of MEX-5.

KEY WORDS: MEX-5, PAR-1, PAR-4, CCCH zinc finger proteins, *C. elegans*

INTRODUCTION

Caenorhabditis elegans embryogenesis begins with a series of polarized divisions that segregate germ cell precursors from cells that produce only somatic cell types (reviewed by Gönczy and Rose, 2005). These divisions result in the asymmetric partitioning of several maternally provided proteins, such as PIE-1, which localizes exclusively to germ cell precursors (Mello et al., 1996). This asymmetric localization is essential for normal development; for example, PIE-1 functions to repress transcription in germ cell precursors, protecting these cells from responding to transcription factors such as SKN-1 that otherwise promote somatic differentiation (Seydoux et al., 1996). Understanding how polarity of the fertilized egg is established, and how this polarity leads to the asymmetric localization of proteins such as PIE-1, are major goals of research in *C. elegans*, and have provided general insights into mechanisms of cell and tissue polarity (for reviews, see Goldstein and Macara, 2007; Gönczy, 2008).

The anteroposterior polarity of the embryo is established at fertilization (Goldstein and Hird, 1996). Sperm entering at the posterior pole initiate waves of cortical contraction that move anteriorly; these events result in an anterior cap of contractile, cortical actomyosin, and a non-contractile posterior domain (for reviews, see Cowan and Hyman, 2007; Marston and Goldstein, 2006). A complex of anterior PAR proteins (PAR-3, PAR-6, PKC-3) accumulates at the anterior cap, at least in part through association with the actomyosin network, while the kinase PAR-1 accumulates in a complementary pattern at the posterior cortex (for reviews, see Goldstein and Macara, 2007; Munro, 2006; Nance, 2005).

[1]Molecular and Cellular Biology Program, University of Washington, Seattle, WA 98195, USA. [2]Division of Basic Sciences, Fred Hutchinson Cancer Research Center, Seattle, WA 98109, USA. [3]Howard Hughes Medical Institute, Seattle, WA 98109, USA. [4]Department of Biology, University of Washington, Seattle, WA 98195, USA.

*Present address: Department of Biology, University of North Carolina at Chapel Hill, Chapel Hill, NC 27599, USA
†These authors contributed equally to this work
‡Author for correspondence (e-mail: jpriess@fhcrc.org)

Accepted 9 September 2008

The cortical asymmetry of the one-cell embryo leads to cytoplasmic asymmetries in mRNA and protein through mechanisms that are not understood, but that require two proteins called MEX-5 and MEX-6 (Schubert et al., 2000). MEX-5 and MEX-6 are highly similar to each other, and, like PIE-1, are dual CCCH zinc finger proteins. However, whereas PIE-1 accumulates in the posterior cytoplasm, MEX-5 and MEX-6 accumulate in the anterior (see Fig. 1A) (Cuenca et al., 2003; Mello et al., 1996; Schubert et al., 2000). The localization of MEX-5/MEX-6 to the anterior is remarkable because the capping of cortical actomyosin creates a countercurrent flow of other cytoplasmic components to the posterior (Hird and White, 1993). *pie-1* mutants have normal, asymmetrical localization of MEX-5, whereas *mex-5;mex-6* double mutants fail to localize PIE-1; embryos depleted of PAR proteins fail to localize both MEX-5 and PIE-1 (Schubert et al., 2000; Tenenhaus et al., 1998). These results suggest a linear pathway, wherein cortical PAR asymmetry establishes cytoplasmic MEX-5/MEX-6 asymmetry, in turn establishing PIE-1 asymmetry. However, mutants depleted of MEX-5 and MEX-6 can have variable defects in PAR localization, indicating a complex interplay between the proteins (Cuenca et al., 2003). Recent studies suggest that MEX-5 affects PIE-1 localization in part by binding the polo kinases PLK-1 and PLK-2 (Nishi et al., 2008). PLK-1 is localized to the anterior of the one-cell embryo in a pattern that is similar to, and dependent on, MEX-5 (Chase et al., 2000; Nishi et al., 2008; Rivers et al., 2008). Both PLK-1 and PLK-2 bind a putative polo-docking site around residue Thr186 in MEX-5; an alanine substitution at Thr186 impairs, although it does not eliminate, MEX-5 function (Nishi et al., 2008).

By the end of the one-cell stage, the fraction of MEX-5 in the posterior cytoplasm is very low, and predominately associated with cytoplasmic granules called P granules (see Fig. 1A) (Schubert et al., 2000). After division, the anterior daughter (high MEX-5, low PIE-1 expression) produces only somatic descendants and is termed a somatic blastomere. The posterior daughter (low MEX-5, high PIE-1 expression) eventually produces germ cells, in addition to somatic cell types, and is termed a germline blastomere. This pattern of unequal cleavage is reiterated in the divisions of the posterior

daughter, producing a succession of new somatic blastomeres with high MEX-5 expression and new germline blastomeres with high PIE-1 expression (Mello et al., 1996; Schubert et al., 2000). In the somatic blastomeres, MEX-5 and residual PIE-1 are eventually degraded by a CUL-2 E3 ligase complex; PIE-1 degradation requires its first zinc finger, and is mediated by the ZIF-1 protein (for zinc finger-interacting protein) (DeRenzo et al., 2003; Reese et al., 2000).

The mechanism that generates MEX-5 asymmetry at the one-cell stage and in successive germline blastomeres is not known. In this report, we identify regions of MEX-5 that are essential for asymmetry. We show that MEX-5 asymmetry is associated with changes in mobility, and that a phosphorylated residue, S458, contributes to this change. Finally, we show that the kinase activities of two PAR proteins, PAR-1 and PAR-4, are required for S458 phosphorylation, and that PAR-dependent phosphorylation of MEX-5 is dynamic and begins during oogenesis.

MATERIALS AND METHODS

Nematode strains and maintenance

The following alleles were used and are described in WormBase (http://www.wormbase.org). LGI: *gsk-3(nr2047)*; LGII: *fzr-1(ok380)*, *mex-6(pk440)* (Schubert et al., 2000), *vrk-1(ok1181)*, *zyg-1(b1)* (Wood et al., 1980); LGIII: *kin-19(ok602)*, *par-2(it5ts)* (Kemphues et al., 1988), *unc-119(ed3)* (Maduro and Pilgrim, 1995); LGIV: *mex-5(zu199)* (Schubert et al., 2000), *mbk-2(ne992)* (Pang et al., 2004), *par-5(it55)* (Morton et al., 2002); LGV: *par-1(b274)*, *par-1(e2012)*, *par-1(it51)*, *par-1(it60)* (Guo and Kemphues, 1995), *par-4(it33)*, *par-4(it47ts)*, *par-4(it75)* (Watts et al., 2000); and transgene *zuIs45* (*nmy-2:NMY-2:GFP*) (Nance et al., 2003).

Plasmid construction and worm transformations

Standard techniques were used to manipulate and amplify DNA; transgenes created for this study are listed in Table S1 in the supplementary material. Constructs containing the *pie-1* promoter and 3′UTR were modified from a *pie-1*:GFP expression vector (Strome et al., 2001), as previously described (Tenlen et al., 2006). *mex-5* promoter constructs contained 4.4 kb of DNA upstream of the initiator ATG, and included 648 bp of the *mex-5* 3′UTR. All site-directed mutagenesis was performed using the QuikChange Site-Directed Mutagenesis Kit (Stratagene). Primer sequences for all constructs are available upon request. Transgenic strains were created by microparticle bombardment of *unc-119* animals as described (Praitis et al., 2001).

Antisera and immunofluorescence

αMEX-5(pS458) was generated by immunizing rabbits with the peptide WTpSEENLGLRGHY (Bethyl Laboratories, Montgomery, TX, USA). The antiserum was affinity purified after pre-clearing with the non-phosphorylated peptide (Bethyl Laboratories), and by ELISA showed >98-fold higher affinity for the phosphorylated peptide. Immunostaining was as described (Leung et al., 1999), with several modifications. Frozen embryos/gonads were incubated in –20°C MeOH for 5 minutes, then in secondary fix [2% paraformaldehyde, 48 mM PIPES, 25 mM HEPES (pH 6.9), 10 mM EGTA (pH 7.5), 2 mM $MgCl_2$] at room temperature for 10 minutes. All washes were done in Tris-Tween (1×Tris, 0.1% Tween-20). Dilutions were as follows: αMEX-5(pS458), 1:1000; αMEX-5, 1:50 (Schubert et al., 2000); αGFP, 1:2000 (Abcam ab6556); αPAR-3, 1:20 (Nance et al., 2003); αPIE-1, 1:20 (Tenenhaus et al., 1998). Incubations were at room temperature for two hours [αMEX-5(pS458), αGFP] or at 4°C overnight.

Protein extracts and western blot hybridization

Embryos were lysed in four volumes of buffer [50 mM HEPES (pH 6.9), 70 mM potassium acetate, 5 mM magnesium acetate, 10% Triton X-100, 1 mM DTT, 10% glycerol, 20 mM β-glycerophosphate, 1 mM PMSF, 0.16 mg/ml Complete-EDTA Free Protease Inhibitors (Roche)] essentially as described (Lamb et al., 1994). Extracts were separated by electrophoresis under reducing conditions using NuPAGE Novex 4-12% Bis-Tris pre-cast gels (Invitrogen), transferred to PVDF membrane (Millipore), and immunostained with αMEX-5 (1:75), αMEX-5(pS458) (1:10,000), or αGFP (1:1000, Roche). Proteins were detected using the ECL western blotting detection reagents, following the manufacturer's instructions (GE Healthcare). For phosphatase treatment, 50 μg of protein was incubated at 37°C with 40 units of alkaline phosphatase (Roche) for 2 hours, and separated on a NuPAGE Novex 7% Tris-Acetate pre-cast gel (Invitrogen).

RNA interference

RNA interference (RNAi) was performed by feeding as described (Kamath et al., 2001; Timmons and Fire, 1998). Strains were from available libraries (Kamath et al., 2001), except for *mbk-2* and *plk-2* (cDNAs yk1696b04 and yk1546g02; Yuji Kohara, National Institute of Genetics, Mishima, Japan), and *mek-2* [480 bp corresponding to exons 1-3 was amplified from genomic DNA by nested PCR, cloned into pPD129.36, and transformed into *E. coli* strain HT115 as described (Timmons and Fire, 1998)]. RNAi against pairs of kinase-encoding genes was performed using the soaking method (Tabara et al., 1998). For *lin-45(RNAi)*, animals were soaked in *lin-45* dsRNA, then allowed to recover for 36 hours on *lin-45* feeding plates before immunostaining.

Confocal imaging and photobleaching

Live imaging was performed on a Nikon TE2000-E stand (Nikon Instruments, Melville, NY, USA), with a 60×, 1.4NA objective lens and controlled by Volocity software (v.4.3.0, Improvision, Waltham, MA, USA). Images were acquired with 491 nm or 561 nm lasers, a Yokogawa CSU-10 confocal spinning disc head equipped with a 1.5× magnifying lens, and a Hamamatsu C9100-13 EMCCD camera (Improvision), with the following settings: exposure time, 200 milliseconds; laser intensity, 85%; camera sensitivity, 165; gain, 1. Photobleaching experiments used the Photonic Instruments Digital Mosaic Photobleaching System (Photonic Instruments, St Charles, IL, USA). For FRAP measurements, anterior and posterior 25 μm^2 regions were photobleached simultaneously for 800 milliseconds at maximum laser power after first acquiring two pre-bleach images; recovery was measured in 15 images (1-second intervals) followed by 3 images (10-second intervals). The image series was exported as a TIFF file, then imported into MetaMorph 7.1.0.0 (Molecular Devices, Downington, PA, USA) as a stack file for data analysis as described previously (Molk et al., 2004). Kymograph analysis was performed in MetaMorph.

For FLIP experiments, a region was drawn with the freehand tool in the posterior quarter of the embryo, then photobleached for a total of 25 iterations with a 50-millisecond laser pulse (~300 mW laser intensity); photobleached embryos developed at least to early morphogenesis stages. Image sequences were exported to MetaMorph; a 400 $pixel^2$ box was drawn in the anterior and posterior of the embryo and in a nearby region for background subtraction. Fluorescence intensity in each box was measured for 25 iterations and exported to a linked Excel spreadsheet (Microsoft, Redmond, WA, USA). Background fluorescence was subtracted from both regions and the fluorescence intensity was plotted.

RESULTS

MEX-5 is expressed in the gonad and distributed uniformly in mature oocytes, but becomes enriched at the future anterior pole of the fertilized egg shortly before first cleavage. (Fig. 1A,B) (Schubert et al., 2000). We refer to the asymmetrical localization of MEX-5 in the one-cell embryo and in later germline blastomeres as MEX-5 asymmetry, and to the degradation of MEX-5 in somatic blastomeres at and after the four-cell stage as somatic degradation. To determine when MEX-5 asymmetry begins, embryos were stained for MEX-5, PAR-3 and DNA. Following oocyte fertilization, the maternally derived chromosomes at the anterior of the embryo rapidly complete both meiotic divisions (Fig. 1C-F). After anaphase II, nuclear envelopes assemble around the paternal (sperm-derived) chromosomes and one set of maternal chromosomes, forming the paternal and maternal pronuclei.

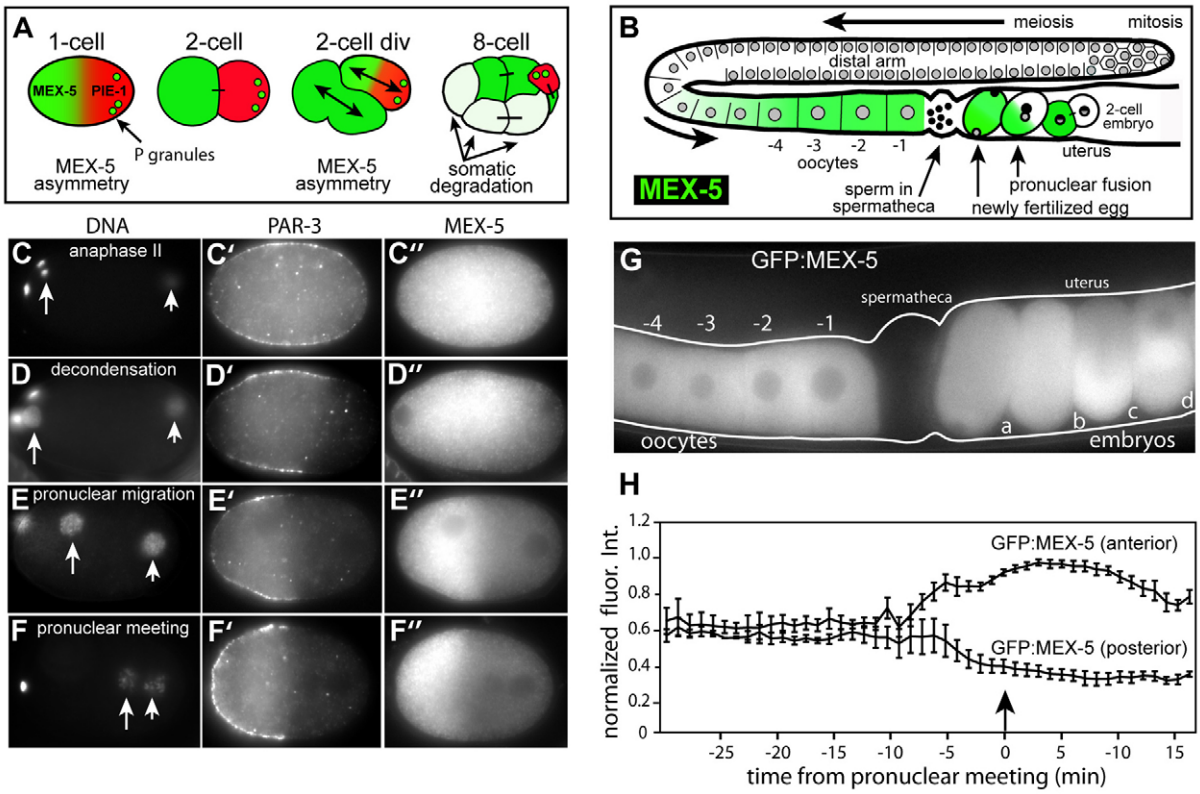

Fig. 1. MEX-5 in oocytes and early embryos. (**A**) Diagram of MEX-5 (green) and PIE-1 (red) localization from the one-cell to eight-cell stages. At the eight-cell stage, the single germline blastomere expresses PIE-1 and the seven somatic blastomeres express MEX-5; somatic degradation is occurring in the four oldest somatic blastomeres (light green; three are visible in this ventral-up orientation). (**B**) Diagram of one arm of the gonad showing germ cells progressing through mitosis, meiosis, and forming oocytes. The oldest oocyte (–1 position) enters the spermatheca where it is fertilized by sperm and pushed into the uterus. (**C-F″**) Each row shows a single one-cell embryo stained for DNA, PAR-3 and MEX-5; arrows indicate nascent maternal (long arrow) and paternal (short arrow) pronuclei. In these wide-field images, fluorescence from cortical PAR-3 is visible in the central focal plane, facilitating comparison with cytoplasmic MEX-5. Anterior is left in all images, and embryos are about 50 μm in length. (**G**) GFP:MEX-5 in the gonad of a live adult. Embryos a-c are at the one-cell stage; a and b are completing meiosis I and II, c is beginning the first mitotic division (posterior up), and d is at the two-cell stage. (**H**) Quantitative fluorescence of GFP:MEX-5 at the anterior and posterior poles of five single embryos recorded before and after pronuclear meeting (arrow) as indicated. Error bars indicate s.e.m.

Chromosomes in both pronuclei decondense, and the maternal pronucleus migrates to the posterior, where it meets and fuses with the paternal pronucleus to form the zygotic nucleus. MEX-5 asymmetry was not detected in any embryos before, or during, anaphase II, but appeared between decondensation and pronuclear meeting (n=0/32 prophase I to anaphase II embryos, 2/7 early decondensation, 7/10 late decondensation, 11/12 pronuclear migration, 17/17 pronuclear meeting; Fig. 1C-F″; see also Movie 1 in the supplementary material). Cortical PAR-3 became asymmetrical at approximately the same time as, or slightly before, MEX-5 asymmetry, and the anteroposterior boundary of PAR-3 expression closely matched that of MEX-5 in all embryos between decondensation and pronuclear meeting (Fig. 1C-F′).

MEX-5 asymmetry requires the zinc fingers and the C-terminus

Transgenes encoding GFP:MEX-5 fusion proteins were generated with the endogenous *mex-5* promoter and 3′UTR, or a heterologous *pie-1* promoter and 3′UTR. Each fusion protein showed the wild-type pattern of expression in oocytes, asymmetry at the one-cell stage and in germline blastomeres, and degradation in somatic blastomeres (Fig. 1G,H; see Movie 1 in the supplementary material); similar observations have been described for GFP:MEX-5 expressed from the *pie-1* promoter and 3′UTR (Cuenca et al., 2003). Live recordings showed that GFP:MEX-5 asymmetry is associated with increased anterior fluorescence and decreased posterior fluorescence (Fig. 1H). The anterior:posterior ratio of GFP:MEX-5 fluorescence at pronuclear meeting was 1.8±0.2, compared with 8.9±2.6 for immunostained, endogenous MEX-5 (n=10; see pJT02 in Fig. 2D). Western blot analysis with anti-MEX-5 and anti-GFP antibodies (hereafter αMEX-5 and αGFP) showed that GFP:MEX-5 was expressed at a much lower level than endogenous MEX-5 (see Fig. 5B). Embryos from *mex-5(zu199);mex-6(pk440)* double mutant adults are inviable (0% hatched, n>100), but most embryos from double mutants expressing GFP:MEX-5 are viable (99% hatched, n=267). Thus, GFP:MEX-5 is expressed at low levels, but provides MEX-5^{+} activity and approximates the wild-type pattern of asymmetry and somatic degradation.

To identify regions of MEX-5 required for asymmetry, transgenes encoding fragments of MEX-5 fused to GFP were generated and integrated into worms (Fig. 2A, see also Table S1 in the supplementary material; and data not shown). Although animals expressing toxic fusion proteins could not have been recovered by our procedures, lines were obtained at comparable frequencies for all but one transgene; we speculate that mutant fusion proteins are tolerated because of the low level of expression. Embryos were scored for

GFP:MEX-5 asymmetry at the one-cell stage (Asym), for association with posterior-localized cytoplasmic granules called P granules (Pg), and for somatic degradation after the four-cell stage (Som; Fig. 2A). N-terminal deletions to residue 199 showed wild-type asymmetry; these deletions remove the T186 residue recently shown to be phosphorylated and important for polo kinase-binding (see Introduction) (see also Nishi et al., 2008). Within the minimal fragment that showed wild-type asymmetry (residues 199 to 468), the region from 199 to 255 appeared to contribute to asymmetry, while two regions were essential for asymmetry: the C-terminal 22 amino acids (pJT45) and a region containing both zinc fingers (ZF1 and ZF2; pJT33).

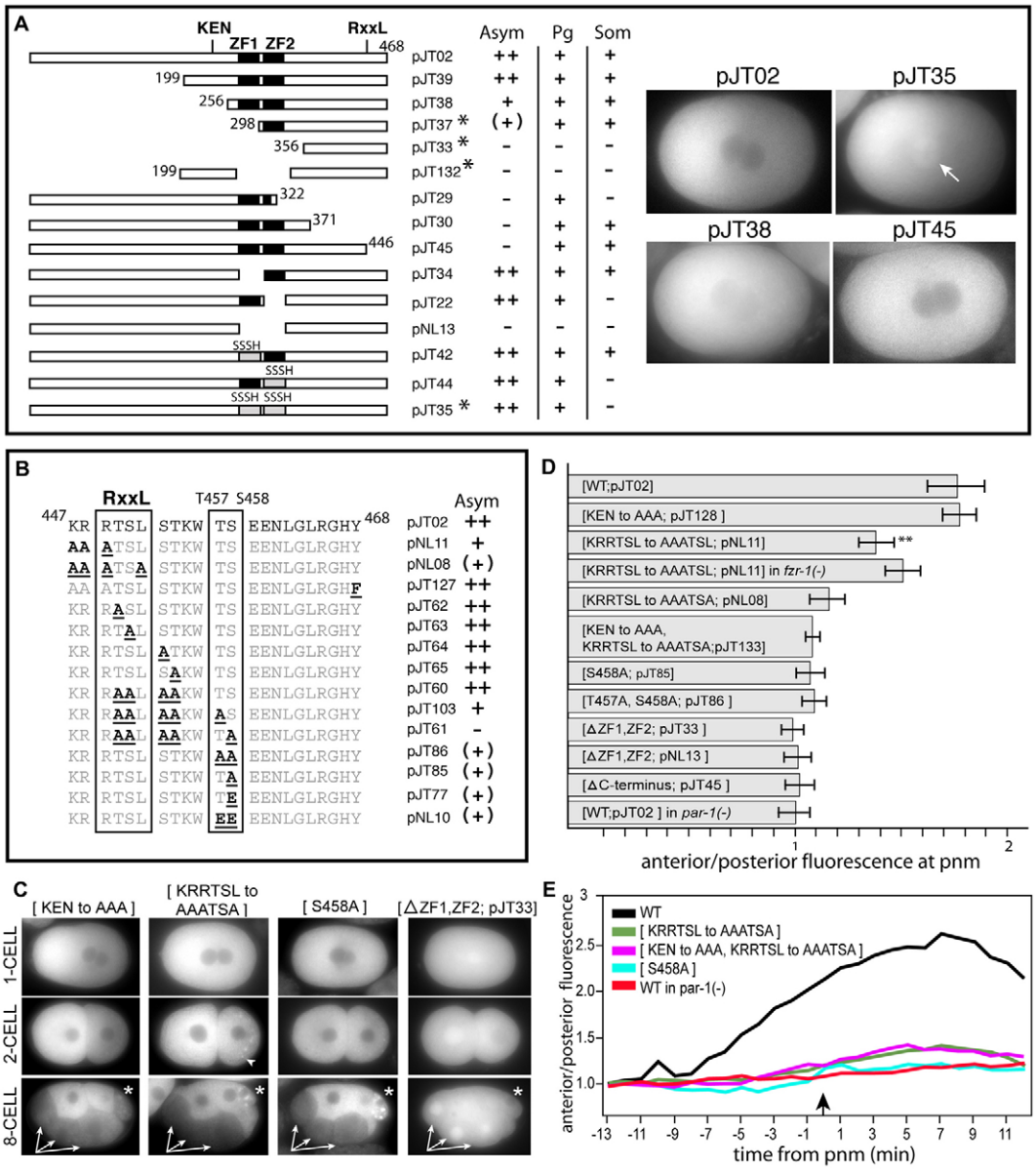

Fig. 2. Regions of MEX-5 required for one-cell asymmetry. (**A**,**B**) Wild-type or mutant MEX-5 proteins were fused to GFP and scored at the one-cell stage for asymmetry (Asym), P granule localization (Pg), and for degradation after the four-cell stage in somatic blastomeres (Som). ++, wild-type asymmetry; +, reduced asymmetry; (+), weak and variable asymmetry; –, no apparent asymmetry. Representative fluorescence images of some embryos are shown in A. Asterisks by plasmid names indicate fusion proteins with prominent nuclear localization in addition to cytoplasmic localization (arrow in image of pJT35). (B) The C-terminal 22 amino acids of MEX-5 indicating substitutions made within full-length MEX-5. (**C**) Fluorescence micrographs of transgenic embryos expressing mutant forms of GFP:MEX-5 as listed, at the one-cell, two-cell and eight-cell stages. The eight-cell-stage embryos are labeled and are in the same orientation as in Fig. 1A; asterisks indicate the germline blastomere P_3. Arrows point to somatic blastomeres at the eight-cell stage, where MEX-5 normally is degraded. GFP:MEX-5$^{KEN\ to\ AAA}$ appeared identical in all respects to GFP:MEX-5 (not shown). The arrowhead points to an example of prominent P granule localization; note abnormally bright P granules in the P_3 cell for S458A. (**D**) Ratio of anteroposterior fluorescence at pronuclear meeting, n>30 embryos each; error bars show s.d., $^{**}P<3\times10^{-4}$ (two-tailed t-test). The type of GFP:MEX-5 fusion protein is indicated in brackets along with the plasmid name. *fzr-1(–)=fzr-1(ok380); par-1(–)=par-1(it51).* (**E**) Ratio of anteroposterior fluorescence in single one-cell embryos expressing GFP fusion proteins and recorded at 1-minute intervals before and after pronuclear meeting (arrow).

Previous studies showed that ZF2 can target a GFP fusion protein for somatic degradation after the four-cell stage, but did not determine whether ZF1 or ZF2 were necessary for somatic degradation, or for MEX-5 asymmetry at the one-cell stage (DeRenzo et al., 2003). We found that ZF2 is essential for somatic degradation, but not for MEX-5 asymmetry, and that ZF1 is not essential for either somatic degradation or MEX-5 asymmetry (pJT22, pJT34; Fig. 2A). However, simultaneous deletion of both ZF1 and ZF2 prevented asymmetry (pNL13, pJT33; Fig. 2A-D). Mutating the zinc finger CCCH residues to SSSH is predicted to disrupt finger structure, and PIE-1 degradation can be prevented by SSSH substitutions in its ZF1 (Reese et al., 2000). SSSH substitutions in the ZF2, but not ZF1, of MEX-5 prevented somatic degradation; however, simultaneous SSSH substitutions in both ZF1 and ZF2 did not prevent asymmetry [Fig. 2A; 100% of one-cell embryos: pJT42 (n=13), pJT44 (n=11), pJT35 (n=8)].

Region 199-255 and the C-terminal 22 amino acids were aligned with corresponding sequences from *C. elegans* MEX-6, and with MEX-5 orthologs in *C. briggsae*, *C. remanei*, *C. brenneri* and *C. japonica* (see Fig. S1 in the supplementary material). These regions contain conserved KEN and KRRTSL sequences, respectively, which are suggestive of KEN-box and RxxL-box motifs that mediate degradation of proteins through the Anaphase-Promoting Complex or Cyclosome (APC/C) (Glotzer et al., 1991; Pfleger and Kirschner, 2000) (reviewed by Zachariae and Nasmyth, 1999). The Fizzy-related/Cdh1 subunit of the APC/C targets KEN- or RxxL-containing substrates for degradation, whereas the Fizzy/Cdc20 subunit targets only RxxL substrates (Fang et al., 1998; Glotzer et al., 1991; Pfleger and Kirschner, 2000). Although little is known about the roles of KEN- or RxxL-boxes in *C. elegans* proteins, the EGG-3 protein contains two RxxL sequences essential for degradation in oocytes (Stitzel et al., 2007).

To test possible roles for KEN and KRRTSL sequences, either or both sequences were mutated within full-length MEX-5 (Fig. 2B-E). Replacing KEN with AAA, or replacing KRRTSL with either KRRASL or KRRTAL had no obvious effect on MEX-5 asymmetry. However, replacing KRRTSL with AAATSL reduced asymmetry, and replacing it with AAATSA markedly reduced asymmetry (Fig. 2B-E). Simultaneously replacing both KEN and KRRTSL with AAA and AAATSA did not further reduce asymmetry (Fig. 2D). Similarly, removing Fizzy-related (FZR-1) function did not further reduce the asymmetry from that seen with the AAATSL substitution (*fzr-1(ok380)* mutants; Fig. 2D). Thus, these experiments do not reveal a role for the KEN sequence in MEX-5 asymmetry, but do indicate a role for KRRTSL within the C-terminal region.

S458 in the C-terminal region is required for MEX-5 function and asymmetry

GFP:MEX-5 fusion proteins and endogenous MEX-5 showed apparent molecular weights in western blots that were larger than expected; treatment with phosphatase reduced the sizes of both bands, indicating that MEX-5 is a phosphoprotein (see Fig. 5A; data not shown). Because two PAR proteins are kinases, and the C-terminal 22 amino acids of MEX-5 include Tyr and several Ser and Thr residues, we investigated whether any of these residues were required for asymmetry. Substituting Ala for five of the Ser and Thr residues simultaneously prevented GFP:MEX-5 asymmetry (Fig. 2B). Although substitutions for most of the individual Ser or Thr residues had no apparent effect, a single S458A substitution markedly reduced asymmetry (pJT85; Fig. 2B-E).

To determine whether S458 was important for MEX-5 function, we used a transgenic strain expressing GFP:MEX-5^{S458A} at a level comparable to the GFP:MEX-5 strain that fully rescues *mex-5(zu199);mex-6(pk440)* mutants (see above). In contrast to our earlier results, none of the mutant embryos expressing GFP:MEX-5^{S458A} was viable (0% hatched embryos, n>200). Previous studies showed that *mex-5;mex-6* double mutants lack PIE-1 asymmetry at the one-cell stage (Schubert et al., 2000). Similarly, PIE-1 was not asymmetric in most double mutant embryos expressing GFP:MEX-5^{S458A} (Fig. 5D; 14/15 embryos showed no PIE-1 asymmetry; 1/15 embryos had weak, reciprocal asymmetry of GFP:MEX-5^{S458A} and PIE-1). Thus, both KRRTSL and S458 within the C-terminal region are important for asymmetry, and S458 at least is essential for MEX-5 function.

MEX-5 asymmetry does not require protein degradation or vectorial transport

We found that the level of GFP:MEX-5 fluorescence integrated over the entire embryo does not change appreciably between decondensation and pronuclear meeting (fluorescence at pronuclear meeting/fluorescence at decondensation=1.01±0.05; n=10 live one-cell embryos). The constant level could mean that MEX-5 is transported to the anterior to create asymmetry. Alternatively, asymmetry could result from ongoing translation of *mex-5* mRNA coupled with KRRTSL-mediated degradation in the posterior. Testing whether general proteasome components, or Fizzy (FZY-1), are required for MEX-5 asymmetry is complicated by the

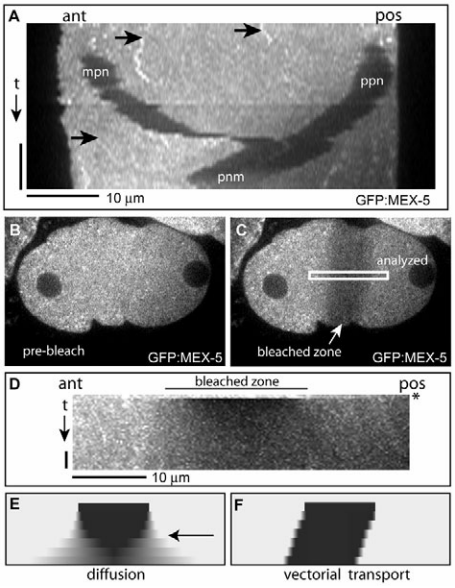

Fig. 3. Kymograph analysis of GFP:MEX-5. (**A**) Kymograph display of images collected from live recording of a one-cell embryo; line widths are 2 microns. Imaging began before the appearance of the maternal and paternal pronuclei (mpn and ppn), when MEX-5 is symmetrical, and ended at pronuclear meeting (pnm), when MEX-5 is asymmetrical. Arrows indicate examples of GFP:MEX-5-containing particles. (**B**,**C**) One-cell embryo as GFP:MEX-5 asymmetry is initiated (decondensation) before (B) and after (C) photobleaching. (**D**) Kymograph of recovery within the boxed zone indicated in C; the asterisk indicates the time point prior to bleaching and line widths are 8.3 microns. (**E**,**F**) Cartoons of idealized kymographs from hypothetical embryos after photobleaching. Scale bars: in A, 4 minutes; in D, 4 seconds.

essential requirement for several of these proteins in meiotic progression preceding MEX-5 asymmetry (Kitagawa et al., 2002; Liu et al., 2004; Shakes et al., 2003; Sonneville and Gönczy, 2004) (for a review, see Bowerman and Kurz, 2006). Indeed, embryos depleted for proteasome components either completed the first mitotic division with normal GFP:MEX-5 asymmetry, or arrested before division with no asymmetry (see Table S2 in the supplementary material). However, if posterior degradation and compensatory translation maintain the constant level of MEX-5, the level of GFP:MEX-5$^{(KRRTSL\ to\ AAATSA)}$ should at least double by pronuclear meeting. Instead, we found no significant change, suggesting that the role of KRRTSL in asymmetry does not depend on degradation (fluorescence ratio=1.03±0.1; n=8 live one-cell embryos).

To examine whether MEX-5 is redistributed to the anterior by vectorial transport, we used kymographs to follow the behavior of small punctae of GFP:MEX-5 that are visible throughout the cytoplasm of one-cell embryos; some, but not all, of the larger particles are P granules (Fig. 3A; see also Movies 1 and 2 in the supplementary material). Numerous punctae moved posteriorly, consistent with previously described cytoplasmic flows (Hird and White, 1993), but few, if any, punctae show sustained movements toward the anterior (Fig. 3A). As a second test, we photobleached GFP:MEX-5 in a large, rectangular zone of cytoplasm prior to pronuclear migration (Fig. 3B,C). If GFP:MEX-5 moves to the anterior vectorially, the posterior end of the bleached zone should recover faster than the anterior; if random movements predominate, both ends should recover symmetrically (Fig. 3E,F). Both ends showed a rapid and similar pattern of recovery, suggesting that GFP:MEX-5 does not move vectorially towards the anterior (Fig. 3D).

We used FRAP (Fluorescence Recovery After Photobleaching) and FLIP (Fluorescence Loss In Photobleaching) experiments to further analyze the mobility of GFP:MEX-5. In the FRAP experiments, small regions in the anterior and posterior of one-cell embryos were bleached simultaneously at, or just after, pronuclear meeting. Recovery of photobleached, control GFP occurred within about 1 second in both the anterior and posterior of the embryo (see Table S3 in the supplementary material), times typical for GFP in other cell types (Sprague and McNally, 2005). By contrast, wild-type GFP:MEX-5 showed an approximately 10-fold slower recovery in both the anterior and posterior of one-cell stage embryos prior to pronuclear migration, suggesting that it has restricted mobility (Fig. 4A; see also Table S3 in the supplementary material). GFP:MEX-5 lacking the zinc fingers domain had fast anterior and posterior recovery times, similar to GFP alone, suggesting that the fingers contribute to the restricted mobility (see Table S3 in the supplementary material).

The relatively slow recovery time of GFP:MEX-5 did not change significantly in the anterior of embryos between decondensation and pronuclear meeting (10.4±1.0 versus 9.2±1.8, respectively; Student's t-test: P>0.05; see Table S3 in the supplementary material). However, the recovery time in the posterior decreased markedly between these stages (10.5±1.6 versus 5.4±0.9; P<0.005; Fig. 4A, Table S3 in the supplementary material). Thus, the development of asymmetry is associated with an apparent increase

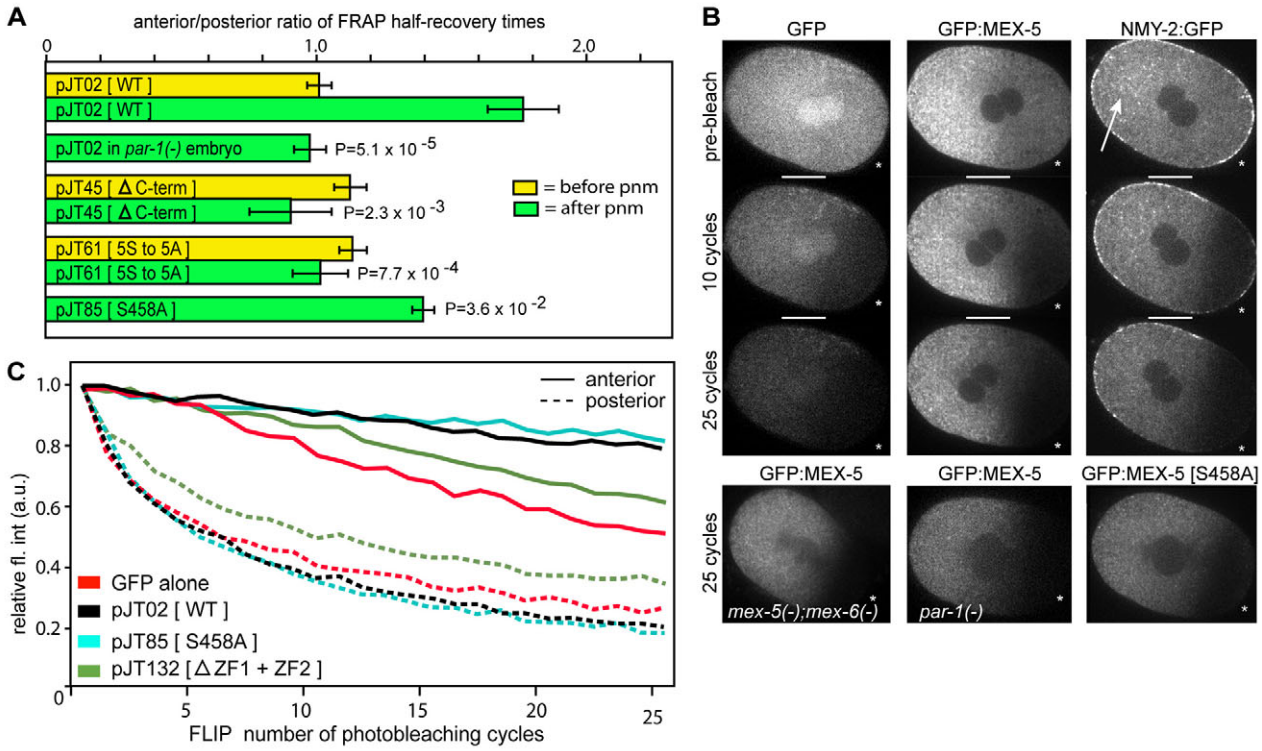

Fig. 4. FRAP and FLIP analysis of GFP:MEX-5 mobility. (**A**) FRAP results on one-cell embryos with GFP or the fusion protein listed (n=4-10 embryos analyzed per experiment). P-values are from comparisons to pJT02 after pronuclear meeting (pnm); error bars show s.e.m. (**B**,**C**) FLIP experiments on embryos at pronuclear meeting. Embryos expressing GFP, NMY-2:GFP, or the GFP:MEX-5 fusion protein listed were photobleached near the posterior pole (asterisk) for the number of cycles indicated. (C) Fluorescence measured at the anterior pole (solid line) and posterior pole (dashed line) for single embryos after each photobleaching cycle for GFP or the GFP:MEX-5 fusion proteins listed. Loss of posterior fluorescence is less for GFP and GFP:MEX-5 [–ZFs; pJT132] than for the other proteins, presumably because a larger fraction of non-bleached, anterior protein moves posteriorly.

in the mobility of posterior MEX-5. This increase did not occur in *par-1(RNAi)* embryos, where MEX-5 fails to develop asymmetry (Schubert et al., 2000), and was dependent on the C-terminal 22 amino acids of MEX-5 (Fig. 4A). Mutating five of the six Ser and Thr residues within the C-terminal region to Ala prevented the increased mobility, and the single S458A mutation had a similar, but more variable, effect on posterior mobility (Fig. 4A).

In FLIP experiments, we analyzed the behavior of anterior GFP:MEX-5 after photobleaching the posterior. If a fluorescent protein in the anterior can move freely into the posterior, repeated photobleaching in the posterior should cause a rapid drop in the level of anterior fluorescence. Indeed, photobleaching posterior GFP, or GFP:MEX-5 lacking both zinc fingers (pJT132), caused the expected rapid drop in anterior fluorescence (Fig. 4B,C; see also Movie 3 in the supplementary material). By contrast, photobleaching posterior GFP:MEX-5 caused only a small decrease in anterior levels, indicating a restriction in the mobility of anterior GFP:MEX-5 (Fig. 4B,C; see Movie 3 in the supplementary material). We observed a similar restricted mobility for anterior GFP:MEX-5 in wild-type oocytes, and in *par-1(it51)* mutant and *mex-5(zu199); mex-6(pk440)* double mutant one-cell embryos (Fig. 4B; data not shown). From these FRAP and FLIP experiments we conclude that GFP:MEX-5 appears to move randomly, but does not diffuse freely in the cytoplasm before fertilization, or in the anterior of embryos after fertilization. The restricted mobility of GFP:MEX-5 requires the zinc fingers, but does not depend on PAR-1^{+} activity or the presence of endogenous MEX-5.

We were interested in the possibility that the actomyosin cytoskeleton might play a role in restricting MEX-5 mobility: During the one-cell stage, the temporal and spatial formation of the anterior cap of cortical actomyosin parallels the cortical localization of PAR-3 (Munro et al., 2004), and hence has a similar anteroposterior boundary to cytoplasmic MEX-5. Consistent with this hypothesis, cytoplasmic NMY-2:GFP (Non-Muscle Myosin-2:GFP) showed a restricted mobility similar to GFP:MEX-5 in FLIP experiments (Fig. 4B). Moreover, NMY-2:GFP appeared in cytoplasmic punctae that were enriched reproducibly in the anterior of the one-cell embryo by the time of pronuclear meeting, suggesting an asymmetry in cytoplasmic actomyosin (arrow in Fig. 4B).

MEX-5 asymmetry requires phosphorylation of S458

The above results show that MEX-5 is a phosphoprotein, that asymmetry is associated with a posterior-specific increase in mobility, and that PAR-1^{+} activity and the C-terminal region, in part through residue S458, are required for the increased mobility. To determine whether S458 is phosphorylated, an antiserum was raised against a synthetic peptide consisting of the C-terminal 13 amino acids of MEX-5, with phospho-Ser458 substituted for Ser458 (see Materials and methods). In western blots of nematode extracts, αMEX-5(pS458) stained a single prominent band at the position of MEX-5, and staining was reduced markedly by treatment with phosphatase, indicating that MEX-5 is phosphorylated at S458 in vivo (Fig. 5A). In extracts from animals containing a GFP:MEX-5 transgene, αMEX-5(pS458) stained bands at about the predicted molecular weights for endogenous MEX-5 and GFP:MEX-5 (Fig. 5B). Conversely, αMEX-5(pS458) stained only endogenous MEX-5 in extracts from either of two transgenic strains expressing GFP:MEX-5^{S458A} (Fig. 5B). αMEX-5(pS458) showed robust staining of a fusion protein lacking both zinc fingers (pJT33; data not shown). However, αMEX-5(pS458) showed little, if any, staining of GFP:MEX-5$^{(KRRTSL\ to\ AAATSA)}$ (Fig. 5C). We conclude that the candidate 'RxxL-box' sequence, but not the zinc fingers, is required for normal levels of S458 phosphorylation.

To determine when MEX-5 is phosphorylated at S458, wild-type embryos and gonads were stained simultaneously with αMEX-5 and αMEX-5(pS458). Both antisera stained *mex-5(+); mex-6(+)* embryos and *mex-5(+); mex-6(–)* embryos, whereas neither antisera

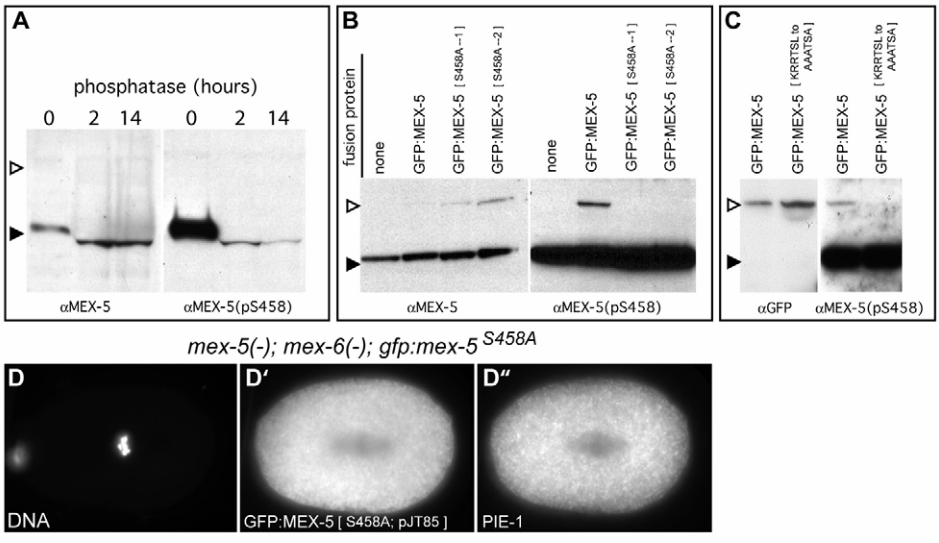

Fig. 5. S458 is phosphorylated and is required for normal embryonic polarity. (**A-C**) Western blots of extracts from wild-type adult worms or worms expressing various GFP:MEX-5 fusion proteins as listed. Black triangles indicate 53 kDa (predicted size of endogenous MEX-5); white triangles indicate 82 kDa (predicted size of GFP:MEX-5). (A) Extracts from wild-type worms treated with alkaline phosphatase for 0, 2 or 14 hours and stained with either αMEX-5 or αMEX-5(pS458). (B) αMEX-5(pS458) stains endogenous MEX-5 but not GFP:MEX-5^{S458A} for two independent lines of worms; compare with levels of GFP:MEX-5 stained by αMEX-5. Note that the levels of all GFP:MEX-5 fusion proteins are much lower than endogenous MEX-5. (C) The GFP:MEX-5$^{(KRRTSL\ to\ AAATSA)}$ fusion protein is stained by αGFP, but not by αMEX-5(pS458). (**D-D″**) Single, transgenic *mex-5(zu199);mex-6(pk440)* embryo expressing GFP:MEX-5^{S458A} and stained for DNA (DAPI, D) and immunostained for GFP (D′) and PIE-1 (D″); embryo is at the one-cell stage and in metaphase of first mitosis.

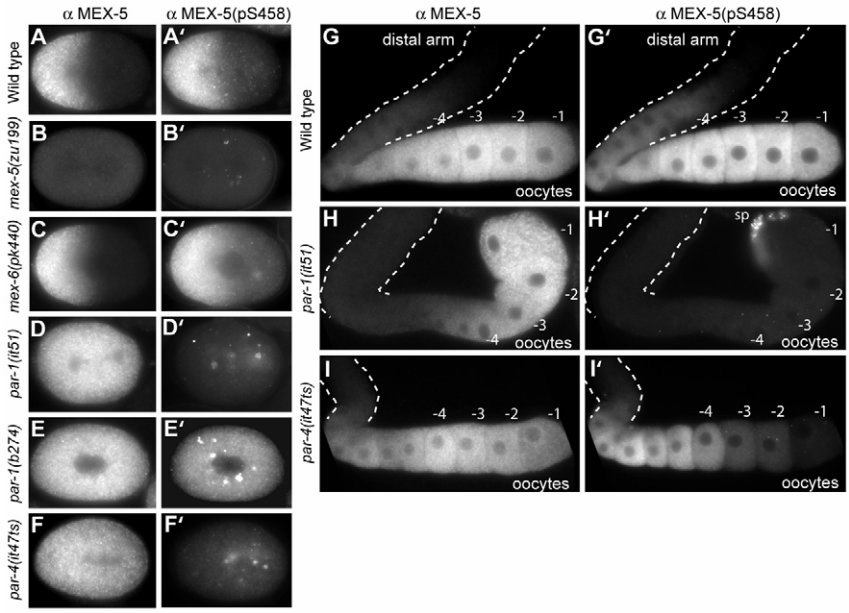

Fig. 6. S458 phosphorylation in embryos and oocytes. (**A-F′**) Each row shows a single one-cell stage wild-type or mutant embryo, as listed after staining with αMEX-5 (left column) and αMEX-5(pS458) (right column). (**G-I′**) Each row shows one arm of a wild-type or mutant gonad, as listed after staining with αMEX-5 (left column) and αMEX-5(pS458) (right column); gonads are oriented as in Fig. 1B. αMEX-5(pS458) shows non-specific staining of cytoplasmic foci in early embryos (B′,D′,E′,F′) and of sperm (sp) in gonads (see H′). *par-1(it51)*, but not *par-1(b274)*, has a mutation in the predicted kinase domain.

stained *mex-5(–); mex-6(+)* embryos (Fig. 6A-C). Combined with our western analysis and ELISA results (see Materials and methods), these results indicate that αMEX-5(pS458) shows a high specificity for MEX-5 phosphorylated at S458. αMEX-5(pS458) showed additional, non-specific staining of sperm (see Fig. 6H′) and cytoplasmic particles in one-cell embryos (Fig. 6B′-F′). Although we anticipated that S458 might be phosphorylated after fertilization, when MEX-5 becomes asymmetric, the staining pattern of αMEX-5(pS458) was instead very similar to that of αMEX-5 in gonads and in early embryos (Fig. 6G,G′). We conclude that S458 phosphorylation is initiated near the time that MEX-5 is first synthesized in oogenesis, and that the phosphorylation level does not change appreciably during the one-cell stage.

PAR-1- and PAR-4-dependent phosphorylation of S458

To identify kinases that phosphorylate MEX-5 at Ser458, we examined 57 predicted serine/threonine kinases that function and/or are expressed in oocytes or early embryos (see Table S4 in the supplementary material). Staining of αMEX-5 and αMEX-5(pS458) was compared in oocytes and early embryos after each kinase was depleted by dsRNA (RNAi) or by available mutations; pairs of closely-related kinases were depleted simultaneously. No differences in staining were observed for 55 kinases. However, depletion of the kinases PAR-1 or PAR-4 resulted in markedly different staining patterns for the two antibodies. Oocytes and one-cell stages with apparently wild-type levels of MEX-5 showed little, if any, staining with αMEX-5(pS458) when *par-1* was depleted by RNAi, or in *par-1(it51)* mutants with a missense mutation in the PAR-1 kinase domain (Fig. 6D,D′,H,H′) (Guo and Kemphues, 1995). By contrast, *par-1(b274)*, *par-1(e2012)* and *par-1(it60)* mutants that do not contain mutations in the kinase domain (Guo and Kemphues, 1995) stained with both antibodies (Fig. 6E,E′; data not shown). Because these three mutants lack MEX-5 asymmetry yet show S458 phosphorylation, PAR-1 must have an additional role in asymmetry that is at least partially separate from S458 phosphorylation. MEX-5 does not contain known PAR-1 phosphorylation sites, and we have not yet been able to determine whether MEX-5 is phosphorylated specifically by PAR-1 (our unpublished results).

Temperature-sensitive *par-4(it47ts)* animals that were grown at the permissive temperature of 15°C showed comparable, wild-type patterns of staining for αMEX-5 and αMEX-5(pS458) (data not shown). αMEX-5 staining did not change noticeably when the animals were raised at the restrictive temperature of 25°C; however, the oldest oocytes and one-cell embryos failed to stain with αMEX-5(pS458) (Fig. 6F,I). Identical results were observed for two non-conditional *par-4* mutants [*par-4(it33)* and *par-4(it75)*], which are predicted to lack PAR-4 kinase activity (data not shown) (Watts et al., 2000). Although MEX-5 contains a candidate PAR-4/LKB1 consensus site in its C-terminus, this site is not required for asymmetry (pJT64 in Fig. 2B). We conclude that PAR-1 kinase activity is required to phosphorylate S458, and that this requirement begins before fertilization. PAR-4 kinase activity is required to maintain S458 phosphorylation in the oldest oocytes just prior to fertilization. PAR proteins in general are not essential for phosphorylation, as S458 was phosphorylated in the following types of embryos: *par-2(RNAi)* and *par-2(it5)*, *par-3(RNAi)*, *par-5(it55)* and *par-5(RNAi)*, and *par-6(RNAi)* (n>20 embryos; data not shown).

DISCUSSION

GFP:MEX-5 in oocytes and early one-cell embryos (before or at decondensation) has a restricted mobility compared with freely diffusible GFP. This difference is vividly illustrated by FLIP experiments, in which anterior GFP:MEX-5 fluorescence is diminished only slowly by repeated photobleaching in the posterior. Although GFP:MEX-5 (82 kDa) is larger than GFP (27 kDa), this size difference alone would not be expected to appreciably impact simple diffusion; FRAP recovery rates for the diffusion of a 100 kDa protein are similar to that of GFP (about 1.5-fold longer) (Sprague and McNally, 2005), while the recovery rate for GFP:MEX-5 is much longer (>10-fold). We found that both ZF1 and ZF2 are required for the restricted mobility of MEX-5, and for MEX-5 asymmetry. Previous biochemical studies on MEX-5, and structural and biochemical studies on CCCH fingers in vertebrate and yeast proteins, have shown that this type of finger binds RNA (Hudson et al., 2004; Kelly et al., 2007; Lai et al., 1999; Pagano et al., 2007). This raises the possibility that association with a target mRNA might restrict MEX-5 mobility; for example, *mex-3* mRNA is enriched in

the anterior half of the one-cell embryo, although *mex-3(RNAi)* does not disrupt MEX-5 asymmetry (Draper et al., 1996; Pagano et al., 2007). However, CCCH to SSSH mutations in both ZF1 and ZF2 of MEX-5 do not prevent asymmetry, whereas even a single mutation in a Cys residue in other CCCH proteins can disrupt RNA binding (Lai et al., 1999).

The behavior of cytoplasmic NMY-2:GFP (non-muscle myosin) in FLIP experiments was similar to that of GFP:MEX-5, suggesting that actomyosin could have a role in restricting MEX-5 mobility. As asymmetry develops, the anterior cap of cortical NMY-2:GFP shows a much sharper anteroposterior boundary than is apparent for cytoplasmic NMY-2:GFP. However, we found that foci of NMY-2:GFP become enriched in the anterior cytoplasm at this stage, suggesting a link between the dynamics of cortical actomyosin and the properties of cytoplasmic actomyosin. Interestingly, yolk and various cytoplasmic granules that flow to the posterior in response to capping of cortical actomyosin move more slowly through the anterior cytoplasm than through the posterior cytoplasm (Hird and White, 1993) (our unpublished results). If a dynamic meshwork of actomyosin extended from the cortex into the deep cytoplasm, it might impede the movement of yolk and other granules in the anterior, as well as restricting MEX-5 mobility (Fig. 7).

The restricted mobility of GFP:MEX-5 does not change appreciably in the anterior of the embryo as asymmetry develops. However, there is an increase in posterior mobility, providing a possible mechanism for the net, anterior accumulation. There are several mechanisms that might explain the increased mobility, such as fewer available binding sites in the posterior, a diminished ability to bind those sites, or both. We showed that the increase in posterior mobility required PAR-1^{+} activity and the C-terminus of MEX-5. Deleting the entire C-terminus or mutating five Ser and Thr residues within the C-terminus caused indistinguishable defects in mobility.

S458 appears to be the most important site in the C-terminus, as mutating this single residue caused a significant, although variable, defect in mobility, and a severe defect in MEX-5 asymmetry. We showed that S458 is phosphorylated in vivo, and that a nearby KRRTSL sequence is required for normal levels of phosphorylation and for GFP:MEX-5 asymmetry. Despite the resemblance of this sequence to the RxxL-box motif involved in APC/Cyclosome-mediated protein degradation, our results indicate that it does not function to degrade GFP:MEX-5. Our analysis indicates that degradation is not essential for asymmetry, but does not exclude the possibility that degradation contributes to the asymmetry of endogenous MEX-5; the level of GFP:MEX-5 is sufficient to rescue *mex-5; mex-6* double mutants, but is much lower than the level of endogenous MEX-5. If the KRRTSL sequence has any functional similarity to an RxxL-box, one possibility is that MEX-5 is a pseudosubstrate of the APC, localizing with the APC and/or competing for binding with other APC substrates. For example, yeast Mad3/BubR1 contains KEN- and RxxL-boxes that mediate binding to the APC subunit Fizzy/Cdc20, but that do not function in degradation (Burton and Solomon, 2007). *C. elegans* FZY-1/Fizzy/Cdc20 is highly asymmetrical in the newly fertilized egg, where it is localized near the maternal chromosomes at the anterior pole during meiosis I (Kitagawa et al., 2002). However, FZY-1 appears to be uniformly distributed at subsequent stages when MEX-5 asymmetry develops (Kitagawa et al., 2002) (our unpublished results).

We found that two kinases that are essential for MEX-5 asymmetry, PAR-4 and PAR-1, are required for S458 phosphorylation. Previous studies with temperature-sensitive *par-4* alleles suggested that the critical period for PAR-4 function begins about 1.5 hours before fertilization (Morton et al., 1992). Because ovulation occurs once every 23 minutes (McCarter et al., 1999), this implies the critical period begins in the –4 oocyte. In gonads lacking PAR-4 activity, the level of phospho-S458 appears normal in early oogenesis, but diminishes between the –4 and –3 oocytes, and is not detectable by fertilization. Thus, the temperature-sensitive period for PAR-4 corresponds to a time when PAR-4^{+} activity is necessary to maintain phospho-S458 in mature oocytes. We do not know whether MEX-5 or MEX-6 have functions in oocytes, although other CCCH finger proteins, such as OMA-1, are present in oocytes and are essential for oocyte maturation (Detwiler et al., 2001). However, the finding that *mex-5(–);mex-6(–)* mutants can have defective localization of the PAR-3/PAR-6/PKC-3 complex (Cuenca et al., 2003) suggests that MEX-5 might have functions before asymmetry is established (see Introduction).

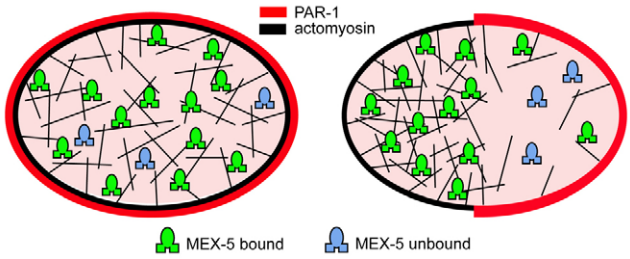

Fig. 7. Model for MEX-5 asymmetry. Speculative model showing MEX-5 before (left) and after (right) asymmetry. MEX-5 is either bound (green) or unbound (blue) to cytoplasmic actomyosin, or to a component whose mobility is limited by actomyosin. Cortical contraction changes the localization, or dynamics, of actomyosin in the deep cytoplasm, such that MEX-5 concentrates in the anterior. Additional sharpening of the MEX-5 asymmetry might come from factors that modulate MEX-5 binding, such as phosphorylation by posterior-localized PAR-1 (red) or non-localized PAR-4 (not shown).

The rapid loss of phospho-S458 in *par-4(–)* mutant oocytes suggests that S458 might not be stably phosphorylated in normal oocytes or embryos, and instead is regulated dynamically by phosphatases and kinases. Consistent with a role for dynamic regulation, we found that substituting a Glu residue for S458, or for both S458 and T457, prevented GFP:MEX-5 asymmetry (see Fig. 2B). Immunostaining experiments with αMEX-5 and αMEX-5(pS458) did not reveal temporally or spatially distinct subpopulations of MEX-5 that lack phospho-S458; however, such experiments do not rule out dynamic changes or microheterogeneity within the cytoplasm. For example, the phosphorylation state of S458 might be involved in the assembly, or disassembly, of MEX-5 protein complexes in mature oocytes, as well as contributing to one-cell asymmetry.

In contrast to the requirement for PAR-4^{+} in mature oocytes, the kinase PAR-1 is required at all stages of oogenesis for S458 phosphorylation. Studies in other systems have shown that the PAR-4 ortholog LKB1 phosphorylates PAR-1 orthologs, and that this phosphorylation is required for PAR-1 kinase activity (Lizcano et al., 2004; Spicer et al., 2003; Woods et al., 2003). By analogy, PAR-4 might function in mature oocytes to maintain the phosphorylated state of PAR-1, which in turn directly or indirectly phosphorylates S458. Whereas PAR-4 is localized uniformly to the cortex and in the cytoplasm of the one-cell embryo (Watts et al., 2000), PAR-1 is restricted to the posterior cortex beginning at about the stage

(decondensation) that MEX-5 first shows asymmetry (Guo and Kemphues, 1995). The *par-1(it51)* allele has a missense mutation in the kinase domain and fails to phosphorylate S458; however, the protein encoded by *par-1(it51)* is expressed at wild-type levels and localizes properly to the posterior cortex (Guo and Kemphues, 1995). Thus, PAR-1 kinase activity, rather than simply localization to the posterior cortex, is required for S458 phosphorylation and MEX-5 asymmetry. Conversely, PAR-1 kinase activity without localization to the posterior cortex is sufficient for S458 phosphorylation, but not for MEX-5 asymmetry: S458 is phosphorylated, but MEX-5 is not asymmetric, in embryos where the wild-type PAR-1 protein is not localized to the posterior cortex [*par-3(RNAi)* embryos]. Similarly, S458 is phosphorylated, but MEX-5 is not asymmetric, in *par-1* mutants that have wild-type kinase domains but lack posterior localization of PAR-1 [*par-1(b274)* and *par-1(e2012)* mutant embryos]. These observations suggest that MEX-5 asymmetry requires both PAR-1 kinase activity and proper localization of PAR-1 to the posterior cortex. In future studies, it will be important to determine whether S458 is phosphorylated, directly or indirectly, by PAR-1 kinase activity during the one-cell stage, or only in early oocytes.

P granule localization and MEX-5 asymmetry

Although most MEX-5 disappears from the posterior prior to first cleavage, a small amount remains associated with P granules; we showed that the zinc fingers are essential for P granule association. For the several types of MEX-5 fusion protein generated in our study that included the zinc fingers, we observed a strong, positive correlation between the level of P granule association and the level of GFP:MEX-5 remaining in the posterior at first cleavage (see Fig. 2C and Movie 2 in the supplementary material). These observations suggest that any MEX-5 that remains in the posterior towards the end of the one-cell stage becomes concentrated in P granules, further lowering the level of free MEX-5. The ability to concentrate posterior MEX-5 on P granules might not be crucial for the one-cell stage, as there is very little posterior MEX-5. However, MEX-5 asymmetry is far less pronounced during the divisions of the later, smaller, germline blastomeres, such as P_3 (Schubert et al., 2000), so it might be important for these cells to sequester posterior MEX-5 in P granules.

We thank Jeremy Nance, Jennifer Schisa, Rafal Ciosk and Kathyrn English for assistance with experimental procedures; these and other members of the Priess lab for valuable discussions; Ken Kemphues for generously providing strains and reagents; and Yuji Kohara (National Institute of Genetics, Mishima, Japan) for providing cDNAs. Some strains used in this study were obtained from the Caenorhabditis Genetics Center, which is supported by the NIH National Center for Research Resources. J.R.T. was supported in part by NIH Training Grant 5T32 HDO7183. J.N.M. was supported by a Postdoctoral Fellowship (PF-08-031-01-CSM) from the American Cancer Society. J.R.P. is an investigator with the Howard Hughes Medical Institute.

Supplementary material

Supplementary material for this article is available at http://dev.biologists.org/cgi/content/full/135/22/3665/DC1

References

Bowerman, B. and Kurz, T. (2006). Degrade to create: developmental requirements for ubiquitin-mediated proteolysis during early *C. elegans* embryogenesis. *Development* **133**, 773-784.

Burton, J. L. and Solomon, M. J. (2007). Mad3p, a pseudosubstrate inhibitor of APCCdc20 in the spindle assembly checkpoint. *Genes Dev.* **21**, 655-667.

Chase, D., Serafinas, C., Ashcroft, N., Kosinski, M., Longo, D., Ferris, D. K. and Golden, A. (2000). The polo-like kinase PLK-1 is required for nuclear envelope breakdown and the completion of meiosis in *Caenorhabditis elegans*. *Genesis* **26**, 26-41.

Cowan, C. R. and Hyman, A. A. (2007). Acto-myosin reorganization and PAR polarity in *C. elegans*. *Development* **134**, 1035-1043.

Cuenca, A. A., Schetter, A., Aceto, D., Kemphues, K. and Seydoux, G. (2003). Polarization of the *C. elegans* zygote proceeds via distinct establishment and maintenance phases. *Development* **130**, 1255-1265.

DeRenzo, C., Reese, K. J. and Seydoux, G. (2003). Exclusion of germ plasm proteins from somatic lineages by cullin-dependent degradation. *Nature* **424**, 685-689.

Detwiler, M. R., Reuben, M., Li, X., Rogers, E. and Lin, R. (2001). Two zinc proteins, OMA-1 and OMA-2, are redundantly required for oocyte maturation in *C. elegans*. *Dev. Cell* **1**, 187-199.

Draper, B. W., Mello, C. C., Bowerman, B., Hardin, J. and Priess, J. R. (1996). MEX-3 is a KH domain protein that regulates blastomere identity in early *C. elegans* embryos. *Cell* **87**, 205-216.

Fang, G., Yu, H. and Kirschner, M. W. (1998). Direct binding of CDC20 protein family members activates the anaphase-promoting complex in mitosis and G1. *Mol. Cell* **2**, 163-171.

Glotzer, M., Murray, A. W. and Kirschner, M. W. (1991). Cyclin is degraded by the ubiquitin pathway. *Nature* **349**, 132-138.

Goldstein, B. and Hird, S. N. (1996). Specification of the anteroposterior axis in *Caenorhabditis elegans*. *Development* **122**, 1467-1474.

Goldstein, B. and Macara, I. G. (2007). The PAR proteins: fundamental players in animal cell polarization. *Dev. Cell* **13**, 609-622.

Gönczy, P. (2008). Mechanisms of asymmetric cell division: flies and worms pave the way. *Nat. Rev. Mol. Cell Biol.* **9**, 355-366.

Gönczy, P. and Rose, L. S. (2005). Asymmetric cell division and axis formation in the embryo. In *WormBook* (ed. The *C. elegans* Research Community), doi/10.1895/wormbook.1.30.1, http://www.wormbook.org.

Guo, S. and Kemphues, K. J. (1995). *par-1*, a gene required for establishing polarity in *C. elegans* embryos, encodes a putative Ser/Thr kinase that is asymmetrically distributed. *Cell* **81**, 611-620.

Hird, S. N. and White, J. G. (1993). Cortical and cytoplasmic flow polarity in early embryonic cells of *Caenorhabditis elegans*. *J. Cell Biol.* **121**, 1343-1355.

Hudson, B. P., Martinez-Yamout, M. A., Dyson, H. J. and Wright, P. E. (2004). Recognition of the mRNA AU-rich element by the zinc finger domain of TIS11d. *Nat. Struct. Mol. Biol.* **11**, 257-264.

Kamath, R. S., Martinez-Campos, M., Zipperlen, P., Fraser, A. G. and Ahringer, J. (2001). Effectiveness of specific RNA-mediated interference through ingested double-stranded RNA in *Caenorhabditis elegans*. *Genome Biol.* **2**, RESEARCH0002.

Kelly, S. M., Pabit, S. A., Kitchen, C. M., Guo, P., Marfatia, K. A., Murphy, T. J., Corbett, A. H. and Berland, K. M. (2007). Recognition of polyadenosine RNA by zinc finger proteins. *Proc. Natl. Acad. Sci. USA* **104**, 12306-12311.

Kemphues, K. J., Priess, J. R., Morton, D. G. and Cheng, N. S. (1988). Identification of genes required for cytoplasmic localization in early *C. elegans* embryos. *Cell* **52**, 311-320.

Kitagawa, R., Law, E., Tang, L. and Rose, A. M. (2002). The Cdc20 homolog, FZY-1, and its interacting protein, IFY-1, are required for proper chromosome segregation in *Caenorhabditis elegans*. *Curr. Biol.* **12**, 2118-2123.

Lai, W. S., Carballo, E., Strum, J. R., Kennington, E. A., Phillips, R. S. and Blackshear, P. J. (1999). Evidence that tristetraprolin binds to AU-rich elements and promotes the deadenylation and destabilization of tumor necrosis factor alpha mRNA. *Mol. Cell. Biol.* **19**, 4311-4323.

Lamb, J. R., Michaud, W. A., Sikorski, R. S. and Hieter, P. A. (1994). Cdc16p, Cdc23p and Cdc27p form a complex essential for mitosis. *EMBO J.* **13**, 4321-4328.

Leung, B., Hermann, G. J. and Priess, J. R. (1999). Organogenesis of the *Caenorhabditis elegans* intestine. *Dev. Biol.* **216**, 114-134.

Liu, J., Vasudevan, S. and Kipreos, E. T. (2004). CUL-2 and ZYG-11 promote meiotic anaphase II and the proper placement of the anterior-posterior axis in *C. elegans*. *Development* **131**, 3513-3525.

Lizcano, J. M., Goransson, O., Toth, R., Deak, M., Morrice, N. A., Boudeau, J., Hawley, S. A., Udd, L., Makela, T. P., Hardie, D. G. et al. (2004). LKB1 is a master kinase that activates 13 kinases of the AMPK subfamily, including MARK/PAR-1. *EMBO J.* **23**, 833-843.

Maduro, M. and Pilgrim, D. (1995). Identification and cloning of *unc-119*, a gene expressed in the *Caenorhabditis elegans* nervous system. *Genetics* **141**, 977-988.

Marston, D. J. and Goldstein, B. (2006). Symmetry breaking in *C. elegans*: another gift from the sperm. *Dev. Cell* **11**, 273-274.

McCarter, J., Bartlett, B., Dang, T. and Schedl, T. (1999). On the control of oocyte meiotic maturation and ovulation in *Caenorhabditis elegans*. *Dev. Biol.* **205**, 111-128.

Mello, C. C., Schubert, C., Draper, B., Zhang, W., Lobel, R. and Priess, J. R. (1996). The PIE-1 protein and germline specification in *C. elegans* embryos. *Nature* **382**, 710-712.

Molk, J. N., Schuyler, S. C., Liu, J. Y., Evans, J. G., Salmon, E. D., Pellman, D. and Bloom, K. (2004). The differential roles of budding yeast Tem1p, Cdc15p, and Bub2p protein dynamics in mitotic exit. *Mol. Biol. Cell* **15**, 1519-1532.

Morton, D. G., Roos, J. M. and Kemphues, K. J. (1992). *par-4*, a gene required for cytoplasmic localization and determination of specific cell types in Caenorhabditis elegans embryogenesis. *Genetics* **130**, 771-790.

Morton, D. G., Shakes, D. C., Nugent, S., Dichoso, D., Wang, W., Golden, A. and Kemphues, K. J. (2002). The *Caenorhabditis elegans par-5* gene encodes a 14-3-3 protein required for cellular asymmetry in the early embryo. *Dev. Biol.* **241**, 47-58.
Munro, E. M. (2006). PAR proteins and the cytoskeleton: a marriage of equals. *Curr. Opin. Cell Biol.* **18**, 86-94.
Munro, E., Nance, J. and Priess, J. R. (2004). Cortical flows powered by asymmetrical contraction transport PAR proteins to establish and maintain anterior-posterior polarity in the early *C. elegans* embryo. *Dev. Cell* **7**, 413-424.
Nance, J. (2005). PAR proteins and the establishment of cell polarity during *C. elegans* development. *BioEssays* **27**, 126-135.
Nance, J., Munro, E. M. and Priess, J. R. (2003). *C. elegans* PAR-3 and PAR-6 are required for apicobasal asymmetries associated with cell adhesion and gastrulation. *Development* **130**, 5339-5350.
Nishi, Y., Rogers, E., Robertson, S. M. and Lin, R. (2008). Polo kinases regulate *C. elegans* embryonic polarity via binding to DYRK2-primed MEX-5 and MEX-6. *Development* **135**, 687-697.
Pagano, J. M., Farley, B. M., McCoig, L. M. and Ryder, S. P. (2007). Molecular basis of RNA recognition by the embryonic polarity determinant MEX-5. *J. Biol. Chem.* **282**, 8883-8894.
Pang, K. M., Ishidate, T., Nakamura, K., Shirayama, M., Trzepacz, C., Schubert, C. M., Priess, J. R. and Mello, C. C. (2004). The minibrain kinase homolog, *mbk-2*, is required for spindle positioning and asymmetric cell division in early *C. elegans* embryos. *Dev. Biol.* **265**, 127-139.
Pfleger, C. M. and Kirschner, M. W. (2000). The KEN box: an APC recognition signal distinct from the D box targeted by Cdh1. *Genes Dev.* **14**, 655-665.
Praitis, V., Casey, E., Collar, D. and Austin, J. (2001). Creation of low-copy integrated transgenic lines in *Caenorhabditis elegans*. *Genetics* **157**, 1217-1226.
Reese, K. J., Dunn, M. A., Waddle, J. A. and Seydoux, G. (2000). Asymmetric segregation of PIE-1 in *C. elegans* is mediated by two complementary mechanisms that act through separate PIE-1 protein domains. *Mol. Cell* **6**, 445-455.
Rivers, D. M., Moreno, S., Abraham, M. and Ahringer, J. (2008). PAR proteins direct asymmetry of the cell cycle regulators Polo-like kinase and Cdc25. *J. Cell Biol.* **180**, 877-885.
Schubert, C. M., Lin, R., de Vries, C. J., Plasterk, R. H. and Priess, J. R. (2000). MEX-5 and MEX-6 function to establish soma/germline asymmetry in early *C. elegans* embryos. *Mol. Cell* **5**, 671-682.
Seydoux, G., Mello, C. C., Pettitt, J., Wood, W. B., Priess, J. R. and Fire, A. (1996). Repression of gene expression in the embryonic germ lineage of *C. elegans*. *Nature* **382**, 713-716.
Shakes, D. C., Sadler, P. L., Schumacher, J. M., Abdolrasulnia, M. and Golden, A. (2003). Developmental defects observed in hypomorphic anaphase-promoting complex mutants are linked to cell cycle abnormalities. *Development* **130**, 1605-1620.
Sonneville, R. and Gönczy, P. (2004). *zyg-11* and *cul-2* regulate progression through meiosis II and polarity establishment in *C. elegans*. *Development* **131**, 3527-3543.
Spicer, J., Rayter, S., Young, N., Elliott, R., Ashworth, A. and Smith, D. (2003). Regulation of the Wnt singalling component PAR1A by the Peutz-Jeghers syndrome kinase LKB1. *Oncogene* **22**, 4752-4756.
Sprague, B. L. and McNally, J. G. (2005). FRAP analysis of binding: proper and fitting. *Trends Cell Biol.* **15**, 84-91.
Stitzel, M. L., Cheng, K. C. and Seydoux, G. (2007). Regulation of MBK-2/Dyrk kinase by dynamic cortical anchoring during the oocyte-to-zygote transition. *Curr. Biol.* **17**, 1545-1554.
Strome, S., Powers, J., Dunn, M., Reese, K., Malone, C. J., White, J., Seydoux, G. and Saxton, W. (2001). Spindle dynamics and the role of gamma-tubulin in early *Caenorhabditis elegans* embryos. *Mol. Biol. Cell* **12**, 1751-1764.
Tabara, H., Grishok, A. and Mello, C. C. (1998). RNAi in *C. elegans*: soaking in the genome sequence. *Science* **282**, 430-431.
Tenenhaus, C., Schubert, C. and Seydoux, G. (1998). Genetic requirements for PIE-1 localization and inhibition of gene expression in the embryonic germ lineage of *Caenorhabditis elegans*. *Dev. Biol.* **200**, 212-224.
Tenlen, J. R., Schisa, J. A., Diede, S. J. and Page, B. D. (2006). Reduced dosage of *pos-1* suppresses Mex mutants and reveals complex interactions among CCCH zinc-finger proteins during *Caenorhabditis elegans* embryogenesis. *Genetics* **174**, 1933-1945.
Timmons, L. and Fire, A. (1998). Specific interference by ingested dsRNA. *Nature* **395**, 854.
Watts, J. L., Morton, D. G., Bestman, J. and Kemphues, K. J. (2000). The *C. elegans par-4* gene encodes a putative serine-threonine kinase required for establishing embryonic asymmetry. *Development* **127**, 1467-1475.
Wood, W., Hecht, R., Carr, S., Vanderslice, R., Wolf, N. and Hirsh, D. (1980). Parental effects and phenotypic characterization of mutants that affect early development in *Caenorhabditis elegans*. *Dev. Biol.* **74**, 446-469.
Woods, A., Johnstone, S. R., Dickerson, K., Leiper, F. C., Fryer, L. G., Neumann, D., Schlattner, U., Wallimann, T., Carlson, M. and Carling, D. (2003). LKB1 is the upstream kinase in the AMP-activated protein kinase cascade. *Curr. Biol.* **13**, 2004-2008.
Zachariae, W. and Nasmyth, K. (1999). Whose end is destruction: cell division and the anaphase-promoting complex. *Genes Dev.* **13**, 2039-2058.